Available online at www.sciencedirect.com
ScienceDirect
Journal of Sound and Vibration 319 (2009) 698–718
JOURNAL OF SOUND AND VIBRATION
www.elsevier.com/locate/jsvi

Constrained adaptive lifting and the CAL4 metric for helicopter transmission diagnostics

Paul D. Samuel*, Darryll J. Pines

Department of Aerospace Engineering, Alfred Gessow Rotorcraft Center, University of Maryland, College Park, MD 20742-3015, USA

Received 16 June 2006; received in revised form 7 June 2008; accepted 9 June 2008
Handling Editor: S. Bolton
Available online 23 July 2008

Abstract

This paper presents a methodology for detecting and diagnosing gear faults in the planetary stage of a helicopter transmission. This diagnostic technique is based on the constrained adaptive lifting (CAL) algorithm, an adaptive manifestation of the lifting scheme. Lifting is a time domain, prediction-error realization of the wavelet transform that allows for greater flexibility in the construction of wavelet bases. Adaptivity is desirable for gear diagnostics as it allows the technique to tailor itself to a specific transmission by selecting a set of wavelets that best represent vibration signals obtained while the gearbox is operating under healthy-state conditions. However, constraints on certain basis characteristics are necessary to enhance the detection of local wave-form changes caused by certain types of gear damage. The proposed methodology analyzes individual tooth-mesh waveforms from a healthy-state gearbox vibration signal that was generated using the vibration separation synchronous signal-averaging algorithm. Each waveform is separated into analysis domains using zeros of its slope and curvature. The bases selected in each analysis domain are chosen to minimize the prediction error, and constrained to have approximately the same-sign local slope and curvature as the original signal. The resulting set of bases is used to analyze future-state vibration signals and the lifting prediction error is inspected. The constraints allow the transform to effectively adapt to global amplitude changes, yielding small prediction errors. However, local waveform changes associated with certain types of gear damage are poorly adapted, causing a significant change in the prediction error. A diagnostic metric based on the lifting prediction error vector termed CAL4 is developed. The CAL diagnostic algorithm is validated using data collected from the University of Maryland Transmission Test Rig and the CAL4 metric is compared with the classic metric FM4.

1. Introduction

In recent years, much research has been devoted to the development of Health and Usage Monitoring (HUM) systems for rotorcraft. The promise of HUM systems is the ability to provide accurate information regarding the condition of various flight critical components. This information would allow scheduled maintenance intervals to be increased and minimize the number of parts decommissioned before the end of

*Corresponding author. Tel.: +1 240 997 1158; fax: +1 301 314 9001.
E-mail address: pdsamuel@gmail.com (P.D. Samuel).

0022-460X/$ - see front matter © 2008 Elsevier Ltd. All rights reserved.
doi:10.1016/j.jsv.2008.06.018

their useful life thus reducing operating costs associated with civilian and military helicopters. In addition, an increase in helicopter safety and reliability could be realized.

A key focus area for much of the HUM system development has been on the use of time–frequency analysis techniques to enhance the salient features present in transmission vibration signatures that are associated with damage. The wavelet transform is one such technique. Unlike the Fourier transform where stationary, complex basis functions are used to map the temporal signal into the frequency domain, a new class of real and complex non-stationary basis functions, termed wavelets, which can be independently dilated and shifted as a function of time, are used to create a unique time–frequency map. The advantage of this method is that the frequency content of the signal can be analyzed in the context of the time domain. It should be noted that the wavelet transform is actually a time-scale technique since complete localization in both time and frequency is impossible according to the uncertainty principle.

Much research has been performed to demonstrate that wavelet analysis is a useful signal processing technique for helicopter transmission diagnostics. An extensive review of this research has been presented by Samuel and Pines [1]. However, finding the manifestation of the wavelet transform that is best suited for diagnostics is an on-going process. Typically vibration signals from both healthy and damaged transmissions are processed using some manifestation of the wavelet transform with a single chosen basis function, the output is analyzed and the ability to identify changes due to damage is reported. The idea behind the use of the wavelet transform with a single basis is that there is one basis function that will allow incipient damage to be detected clearly and consistently. Thus, all that is required is an exhaustive study of all basis functions in order to find the single most effective basis function.

However, current research suggests that the best solution may not be in the use of a single basis, but instead in the use of a set of bases that best represent or model individual components of the signal [2–5]. As with most model-based diagnostic techniques, the general diagnostic approach consists of two stages.

(1) *Offline*: Collect baseline vibration data from the transmission of interest operating under nominal, healthy conditions, termed *healthy-state* conditions. Generate an empirical model based on this data.
(2) *Online*: Collect vibration data from the transmission during normal operating conditions, termed *future-state* conditions. Employ some technique to compare the model with the future-state vibration signals and assess the difference between the model and the signal to determine whether damage is present.

The fundamental idea is if a healthy signal is used to generate the model, then future healthy signals will yield small errors when compared to the model while damaged signals will yield larger errors. This approach is facilitated by the advent of adaptive signal-processing techniques.

In this approach, the wavelet transform is no longer being used to explicitly provide frequency information as a function of time. Instead, the basis functions are used to model the signal in the time domain. The chosen set of bases act as a model of the signal, and the error between the model and future-state signals is analyzed. The wavelet transform offers a known framework in which to perform signal modelling and analysis. However, since the signals are being modelled in the time domain, a time domain realization of the wavelet transform is desired. This time domain manifestation of the wavelet transform is termed the lifting scheme [6]. The lifting scheme is a time domain prediction-error realization of the wavelet transform.

Methods for adding adaptivity to the lifting scheme have begun to be investigated [7,8]. The method used in this work is based on that developed by Claypoole et al. [8]. However, it has been found that adaptive lifting by itself is too flexible to allow the effective distinction of healthy- and damaged-state vibration signals. Hence, it has been determined that constraints on certain basis characteristics are necessary to enhance the detection of local waveform changes caused by certain types of gear damage. This processing technique is termed constrained adaptive lifting (CAL).

This paper suggests a diagnostic approach based on the time domain analysis of the individual tooth mesh waveforms using a signal adaptive time domain realization of the wavelet transform. First, the analysis of the individual tooth mesh waveforms is discussed. The theory behind the lifting scheme is given and adaptive lifting is discussed. CAL is then presented as a means to enhance observed changes in the vibration signal associated with the onset of individual tooth damage and a metric referred to as CAL4 is developed.

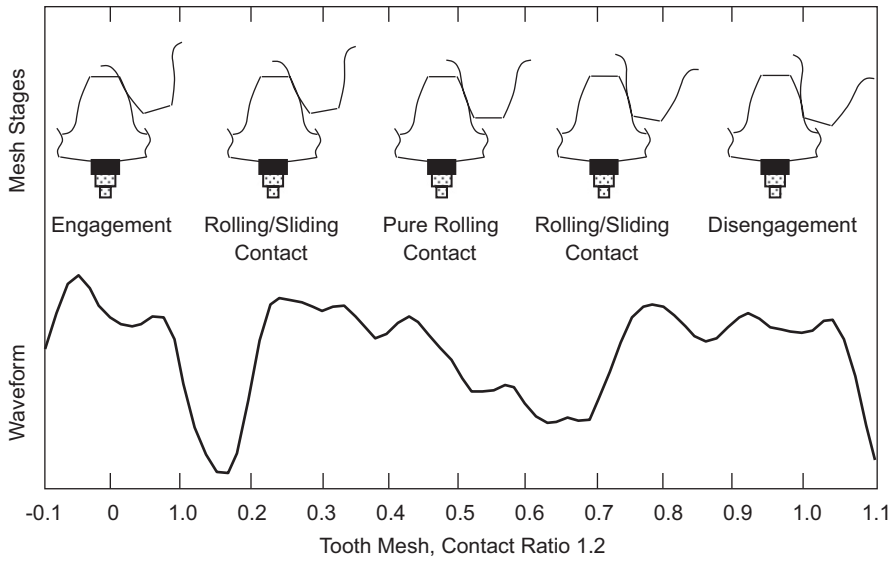

Fig. 1. Stages of conjugate action and associated tooth mesh waveform vibration signal from accelerometer.

To validate the methodology, healthy- and damaged-state data was collected from a planetary transmission test rig, the University of Maryland Transmission Test Rig (UMTTR).

2. Tooth mesh waveform analysis

It has been shown that the vibration waveform associated with a single tooth mesh period has a consistent underlying structure [5,9]. A typical waveform collected from an accelerometer and the associated stages of the conjugate action of a pair of meshing teeth (only approximately associated) are shown in Fig. 1.

Although researchers are investigating high fidelity tooth mesh models to accurately predict gear vibration signals [10,11], no analytical model of the conjugate action of a pair of teeth currently exists that can consistently predict expected vibration waveforms as measured by an accelerometer of both healthy and damaged gears with a sufficient fidelity to be used for diagnostics. However it has been shown that the waveform is well approximated experimentally by the time synchronous average of the raw vibration signal [9,12]. In addition, damage on a single tooth, in particular face damage, causes changes in the shape of the tooth mesh vibration waveform. Thus, a model-based diagnostic approach is suggested where a modelling and analysis is performed at the level of the individual tooth mesh waveform.

3. The lifting scheme

The lifting scheme was developed by Sweldens in the early 1990s as a method for creating new biorthogonal wavelets in settings where the Fourier transform could not be used [6,13,14], such as on bounded domains and on curves and surfaces. Connections are cited between lifting and other independent research, particularly the work of Herley and Vetterli [15]. In later work, Sweldens and Daubechies presented a formal, mathematically rigorous description of lifting, and demonstrated that all perfect reconstruction filterbanks could be formed with a sequence of lifting steps [16].

The lifting scheme is a time-domain prediction-error realization of the wavelet transform, and provides a convenient framework for the implementation of new wavelet-based signal analysis techniques. In addition, the lifting scheme is easily modified for use in specific application areas with specific requirements, making it a prime candidate for the development of advanced wavelet-based signal modelling diagnostic techniques. A simplified presentation of lifting focusing primarily on the implementation and mechanics of the transform is given in this section.

The fundamental idea behind the wavelet transform is to create a sparse approximation of a given signal using a set of basis functions that exploit the correlation present in the signal. The result of the transform is an approximation of the signal and a measure of the difference between the approximation and the original signal, referred to as the detail. The classical wavelet transform takes advantage of the Fourier transform to construct this approximation in the frequency domain. Lifting achieves the same result while operating exclusively in the time domain. A lifting step consists of three stages: split, predict, and update. Consider a signal $x = (x_l)$ with $x_l \in \mathbf{R}$ where $l \in \mathbf{Z}$ is the sample index.

Split: The splitting stage separates the signal into two disjoint sets $\mathbf{x}_e = (x_{2l})_{l\in\mathbf{Z}}$ and $\mathbf{x}_o = (x_{2l+1})_{l\in\mathbf{Z}}$, consisting of the even and odd indexed samples, respectively. This process is termed the polyphase transformation and the resulting sets are referred to as polyphase components of signal x.

Predict: The prediction stage attempts to use $\mathbf{x}_o$ to predict $\mathbf{x}_e$ as

$$\mathbf{x}_e = P(\mathbf{x}_o), \tag{1}$$

where P is the prediction operator (predictor). The difference between the predicted and actual $\mathbf{x}_e$ is called the detail $\mathbf{d}$ and is given by

$$\mathbf{d} = \mathbf{x}_e - P(\mathbf{x}_o). \tag{2}$$

In general, the predictor is designed to suppress the low-order polynomial signal structure within the detail while preserving the high-order structure. This is equivalent to preserving the high-frequency signal structure. For example, let the prediction operator be first order (linear) polynomial interpolation. This is referred to as an $N = 2$ point prediction since two points from $\mathbf{x}_o$ are used to predict the point of $\mathbf{x}_e$ under consideration. The predictor is then given as

$$P(\mathbf{x}_o) = \tfrac{1}{2}(x_{j,2l-1} + x_{j,2l+1}), \tag{3}$$

where j is the dilation index. The resulting detail is given as

$$d_{j-1,l} = x_{j,2l} - \tfrac{1}{2}(x_{j,2l-1} + x_{j,2l+1}). \tag{4}$$

Thus, in this case, the detail is the extent to which the signal fails to be linear.

Update: Finally, in order to maintain acceptable frequency characteristics in $\mathbf{x}_o$, it is necessary to reduce the effect of aliasing introduced by the polyphase transformation. The update operator U uses $\mathbf{d}$ to preserve some frequency properties of x in $\mathbf{x}_o$. In practice, U serves to smooth $\mathbf{x}_o$. The resulting signal, referred to as the approximation $\mathbf{a}$, is given by

$$\mathbf{a} = \mathbf{x}_o + U(\mathbf{d}). \tag{5}$$

The update operation serves to suppress the high-order polynomial signal structure within the approximation, while preserving the low-order structure, which is equivalent to preserving the low-frequency signal structure. Returning to the example, the update operator is given as

$$U(\mathbf{d}) = \tfrac{1}{4}(d_{j-1,l-1} + d_{j-1,l}). \tag{6}$$

This is an $\tilde{N} = 2$ point update. The approximation is thus given as

$$a_{j-1,l} = x_{j,2l+1} + \tfrac{1}{4}(d_{j-1,l-1} + d_{j-1,l}). \tag{7}$$

In this case, the update operator preserves the average of the original signal in the approximation.

If the prediction and update operators are restricted to be translates and dilates of a single function, then the approximation and detail resulting from one lifting step are equivalent to the approximation and detail produced by one step of the wavelet transform. For example, in the case presented above, the linear predict/average preserve implementation of the lifting scheme is equivalent to the biorthogonal (2,2) wavelet transform of Cohen–Daubechies–Feauveau [17].

The block diagram describing one step of the lifting decomposition is given in Fig. 2. To generate a multi-scale representation of a given signal, an iterative approach is used where the split, predict, and update steps are applied to the approximation resulting from the previous iteration. The result is the time-scale representation that can be used to investigate the joint time–frequency characteristics of the signal. This

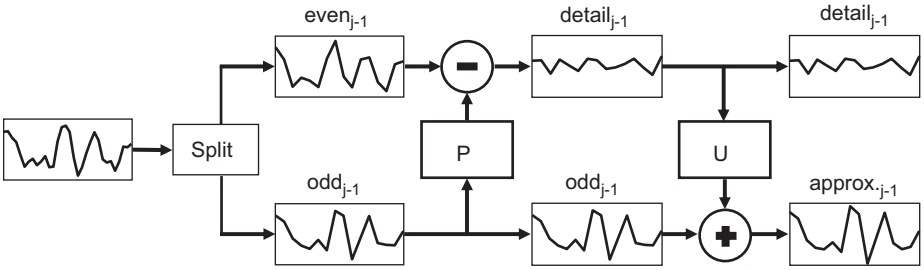

Fig. 2. The lifting scheme block diagram.

representation is the same as that resulting from the traditional wavelet transform when the same basis function is used.

4. Adaptive lifting

It has been proposed that a wavelet system that uses multiple bases to shape itself to the signal could be more effective than the classical wavelet transform for transmission diagnostics. This set of basis functions is termed a *dictionary*. Typically a dictionary is over-complete and non-unique since some elements can be represented in terms of other elements. Thus, many different representations of a given signal are possible, and some method must be employed to select the representation that is in some sense best. The selection of a best representation is referred to as adaptation and amounts to the creation of a small, refined dictionary from a large over-complete dictionary. Adaptation enables the creation of a general diagnostic algorithm that is able to adapt itself to a specific transmission. More specifically, if a set of wavelet basis functions can be selected that best represent a vibration signal obtained from a given transmission operating under healthy-state conditions, then the bases can act as an empirical model of vibration signal. The damage detection algorithm should be less sensitive to any vibration characteristics unique to that transmission. Accordingly, the algorithm should be more sensitive to changes in the vibration signal associated with damage. Adaptive lifting provides a method by which dictionaries tailored to a specific data set can be created.

A number of methods for obtaining signal representations in over-complete dictionaries have been developed in recent years. These include the Method of Frames [18], Best Orthogonal Basis [19], Matching Pursuit [20], and Basis Pursuit [21]. The result is a method for obtaining signal representations that is significantly more flexible than the classical wavelet transform. In addition, the resulting representations should be more sparse and thus more physically meaningful than typical wavelet transform representations.

The key to adding adaptivity to the lifting scheme lies in the method by which the prediction operator P is chosen. In classical lifting, the chosen predictor remains constant. This is equivalent to using a single wavelet basis. However, to incorporate adaptivity, it is necessary to allow the predictor to vary such that the resulting representation is locally optimal in some sense. Some research into the development and application of adaptive lifting algorithms has been initiated [7,8,22,23]. However, the development presented herein is based on the work of Claypoole et al. [8].

In 1998, Claypoole et al. [8], presented a method for adapting the predictor referred to as the Space-Adaptive Transform (SpAT). Recall that in the above example the prediction operator is linear interpolation. The fundamental idea behind the SpAT is that higher order interpolating polynomials are also considered at each point in the signal, and the polynomial that provides the best prediction (minimum prediction error) at a given point is chosen as the prediction operator at that point. In the study reported in Ref. [8], the SpAT is implemented using an $\tilde{N} = 1$ update in conjunction with an $N \in \{1, 3, 5, 7\}$ point prediction, which leads to the biorthogonal $(1, N)$ wavelet bases of Cohen–Daubechies–Feauveau [17].

5. Constrained adaptive lifting

In general, an adaptive signal representation is formed by considering every basis in the dictionary, and the basis which in some manner best represents the signal at a given point is selected. This type of adaptation is

herein referred to as *unconstrained adaptation*, since all bases are considered for every point in the signal. A diagnostic technique based on unconstrained adaptation was developed by Samuel and Pines [24]. It was found that in many cases, unconstrained adaptation yields a model that is too flexible to allow the effective distinction of healthy- and damaged-state vibration signals.

However, the SpAT technique presented by Claypoole, et al. [8] incorporated an additional requirement for the selection of the best basis so that points across a sharp edge which were not strongly correlated to the point under consideration were not used in the predict stage. Thus smooth parts of the signal were modelled using smooth, high-order functions, while edges were modelled using a step function.

This type of adaptation is referred to as *constrained adaptation*. Thus, an adaptive signal processing technique based on lifting and incorporating some form of constraints can be referred to as CAL.

5.1. Adaptation constraints for transmission diagnostics

It has been observed that certain types of gear damage, specifically tooth face damage, can yield higher order changes in the vibration signal waveform. Fig. 3 shows the effect of tooth face spalling on the waveform of an individual tooth mesh.

Thus the first constraint is suggested. The lowest order basis function which sufficiently models the signal at a given point, i.e. the lowest order polynomial that produces a prediction error within some tolerance of the minimum prediction error, should be chosen. The tolerance must be chosen through experimentation. By reducing the basis function order, the model becomes inflexible to higher order changes in the shape of subsequent signals under analysis.

In order to assist the technique in the selection of the lowest order polynomial, a second constraint is suggested. The signal should be separated into analysis domains based on slope inflection points. Specifically, the signal should be divided into separate domains bounded by the slope inflection points, and subsequent analysis should be performed exclusively within each domain. Within each domain the function will effectively be monotonic. However, each tooth mesh waveform to be analyzed is only an approximation of the underlying vibration signal due to averaging. In addition, each of the tooth mesh waveform tends to span only a very short period of time, and thus is represented by a relatively spares set of samples when a reasonable sampling rate is used. Thus some approximate method for determining the location of the slope inflection points is desired. The smoothing spline of Schoenberg and Reinsch [25] provides a convenient method for approximating the tooth mesh waveform with a differentiable function.

Once the analysis domains have been determined, a single spline is used as the predictor within each domain to increase the rigidity of the prediction function to changes in the shape of the signal. Least squares spline

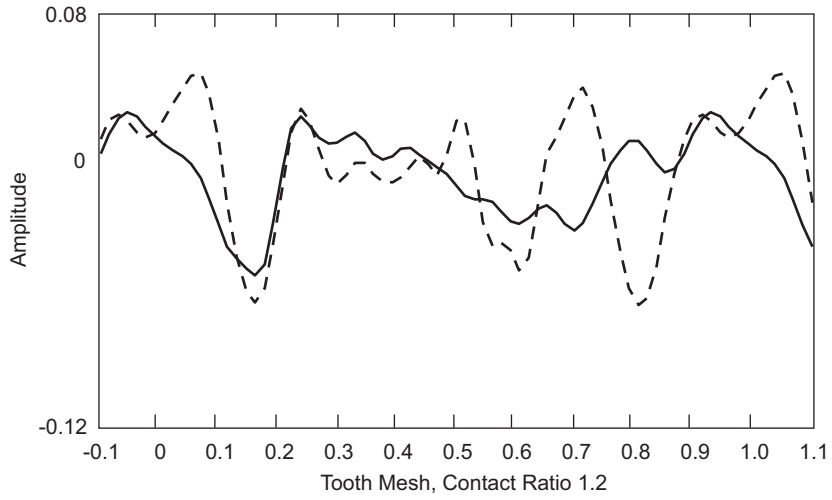

Fig. 3. Effect of tooth face damage on tooth mesh waveform vibration signal from accelerometer (amplitude in volts). ——, No damage; - - -, spalled tooth.

approximation [26] provides a convenient technique for the selection of an approximate predictor function. The number of knots used by the spline is set equal to the number of curvature inflection points of the smoothing spline within the domain plus one additional knot for each endpoint. This allows the spline to account for changes in curvature within the domain. Thus both the order of the spline predictor and the number and location of the knots are constrained. To summarize, two primary constraints are suggested.

(1) The individual tooth mesh waveform is divided into analysis domains based on the slope inflection points of a healthy-state transmission vibration signal. The domains are fixed and used for subsequent analysis of future-state vibration signals. Lifting occurs only within each domain.
(2) The predictor P is constrained to be the lowest order least squares spline approximation that provides a sufficiently small prediction error for a healthy-state transmission vibration signal. Both the order and the knots are fixed for the analysis of future-state vibration signals.

The goal of these constraints is to divide the tooth mesh waveform into simple, effectively monotonic functions, so that they can be approximated by low-order spline functions. This should make the resulting model rigid to the appearance of higher order features associated with damage, thus yielding large prediction errors.

5.2. The smoothing spline for domain selection

In order to find the slope and curvature inflection points of the tooth mesh waveform, a smoothing spline must be generated based on the waveform. The technique for constructing the smoothing spline f for a specified smoothing parameter p was presented by Reinsch in 1967 [25]. Once the spline is found, it can be differentiated and twice differentiated to find the slope and curvature inflection points of the signal.

For the transmission diagnostic algorithm, the smoothing parameter p, which serves to set the tolerance of the spline following the actual data, is chosen such that the greatest number of domains are created while avoiding single point domains. As the tolerance is tightened, the smoothing spline more closely follows the data, and small variations can lead to changes in slope and curvature. Thus a tighter tolerance yields a larger number of domains. However, increasing the number of domains decreases the number of samples within each domain. Analysis cannot be performed on a domain containing a single sample. Thus, the tolerance is reduced until a single point domain is encountered. At this point the tolerance is fixed and each analysis domain is extended by one sample on each edge of the domain. Thus, the smallest domain contains 3 samples which is sufficient for analysis. Note that this technique results in some overlap between domains. This is allowed given the approximate nature of the signal under consideration.

Fig. 4 shows a representative tooth mesh waveform and the six analysis domains formed using the slope inflection points. Let each domain be denoted by the index $\beta \in \mathbf{Z}$ with $\beta = 1, \ldots, N$ where N is the number of domains. Thus in the example shown in Fig. 4, $N = 6$. Note that the tolerance on the selected smoothing spline appears to be insufficient to capture the characteristics of the signal in domain $\beta = 5$, and as a result, the signal in domain $\beta = 5$ may not be sufficiently monotonic. This suggests that a time-varying tolerance, implemented using a time-varying weight vector, may improve the fidelity of the modelling process. However, the selection of an appropriate weight vector is a non-trivial task [27] and is suggested as a topic of future research.

5.3. Least squares spline approximation for basis selection

In order to select the predictor spline within each domain, least squares spline approximation is used [26]. Least squares approximation is the best possible approximation with respect to a discrete inner product. The number of knots is set equal to the number of curvature inflection points plus one for additional knot for each endpoint. An acceptable set of knot locations is selected such that the Schoenberg–Whitney conditions are fulfilled.

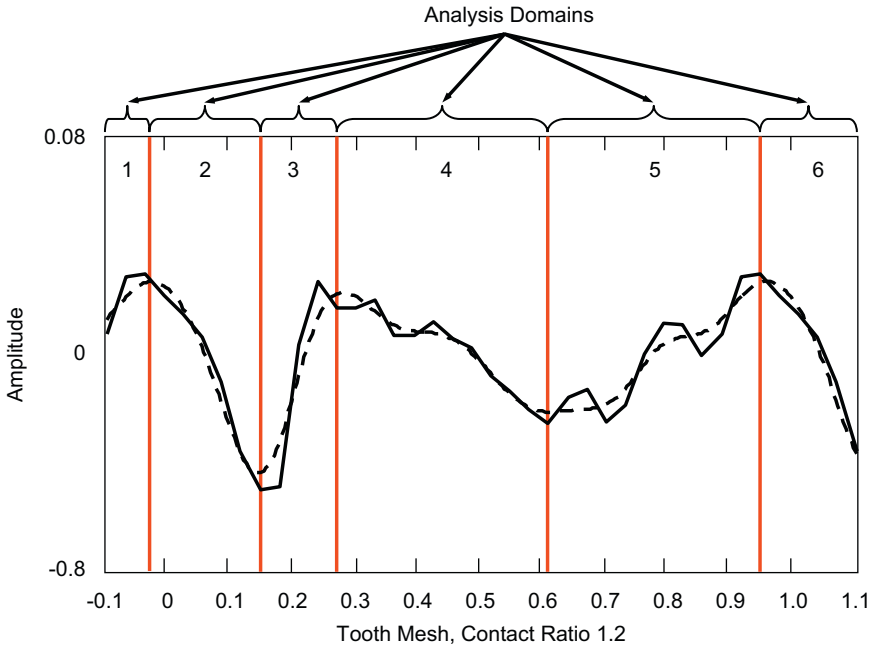

Fig. 4. Tooth mesh waveform vibration signal from accelerometer (amplitude in volts) with analysis domains indicated. ——, Vibration data; - - -, smoothing spline with tolerance = 0.005.

Consider domains $\beta = 4$ and 5 in Fig. 4. Least squares spline approximation of orders 1–6 are used to form the predictors. The prediction error is then assessed. This error is given for each domain in Fig. 5 along with the designated error bound of width 0.001 about the minimum error.

Note that in the domain $\beta = 4$, the fifth-order predictor easily out performs the others, and is subsequently chosen. In the domain $\beta = 5$, the minimum prediction error is given by the sixth-order predictor. However, the fourth-order predictor falls within the designated error bound, i.e. it provides a sufficiently small prediction error. Thus the fourth-order predictor is selected. The polyphase components $\mathbf{x}_o$ and $\mathbf{x}_e$ along with the chosen predictor for domains $\beta = 4$ and 5 are shown in Fig. 6. Let the prediction error vector for domain β be given as ρ_β. Then φ is the complete CAL prediction error vector for a given tooth formed by concatenating the ρ_β.

5.4. Constrained adaptive lifting diagnostic algorithm

Given the stated constraints, an algorithm for transmission diagnostics using CAL can now be presented. The algorithm consists of two procedures. The first is an offline procedure that is performed prior to or at the beginning of in-service operation. The second is an online procedure that is performed during in-service operation.

Offline, the methodology analyzes individual tooth-mesh waveforms from a healthy-state gearbox vibration signal. First, the polyphase transform is applied to each waveform. The zeros of the first derivative (slope) and second derivative (curvature) of the polyphase component $\mathbf{x}_o$ are approximated using a smoothing spline. The slope inflection points are used to designate the analysis domains over which the slope remains approximately constant, and the curvature inflection points within each domain are recorded for subsequent use. The minimum feasible tolerance for the smoothing spline is selected.

Once the analysis domains have been determined, the predictor is chosen as the lowest order least squares spline approximation of the polyphase component $\mathbf{x}_o$ that effectively minimizes the prediction error in the l_2 sense. The number of curvature inflection points within each domain are used to set the number of knots for the spline. The result of the modelling process is a set of analysis domains, each with an associated spline order and set of knots.

Online, future-state vibration signals are divided into the predetermined analysis domains and lifting is then performed within each domain using a least squares spline approximation of predetermined order and knots

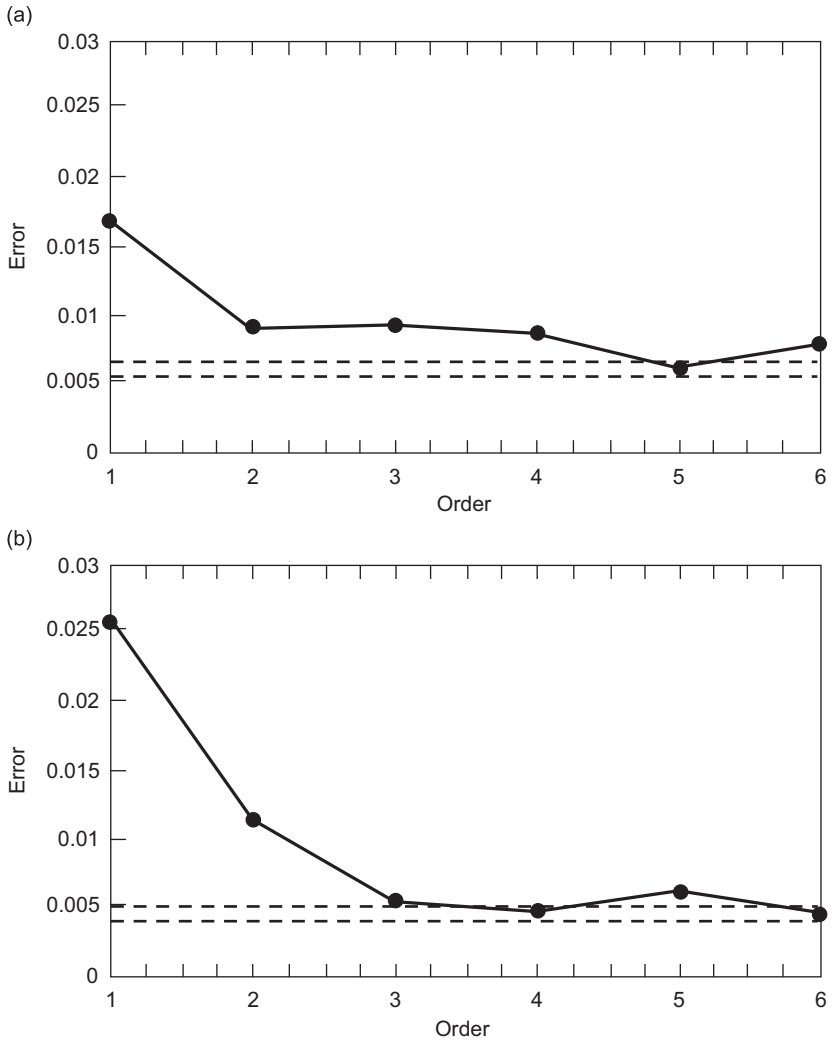

Fig. 5. Prediction error (amplitude in volts): (a) domain 4 and (b) domain 5. ●—●, Prediction error; - - -, error bound.

as the predictor. The resulting prediction error vector for each domain, ρ_β, is inspected for indications of damage. Specifically, it is expected that large prediction errors will be associated with tooth face damage. It should be noted that, for this algorithm, the detail resulting from a single lifting step is the primary result of interest, and thus the update is disregarded.

5.5. Diagnostic metric CAL4

In order to compare the output of the CAL diagnostic algorithm with the various damage detection metrics, a method to quantify the CAL prediction error vector output is desired. Consider the classic damage detection metric FM4 developed by Stewart in 1977 [28], given as

$$\mathrm{FM4} = \frac{N\sum_{i=1}^{N}(d_i - \bar{d})^4}{[\sum_{i=1}^{N}(d_i - \bar{d})^2]^2}, \tag{8}$$

where d is the difference signal formed by subtracting the mesh frequency and harmonics as well as the corresponding first-order sidebands of the gears under consideration from the experimentally obtained

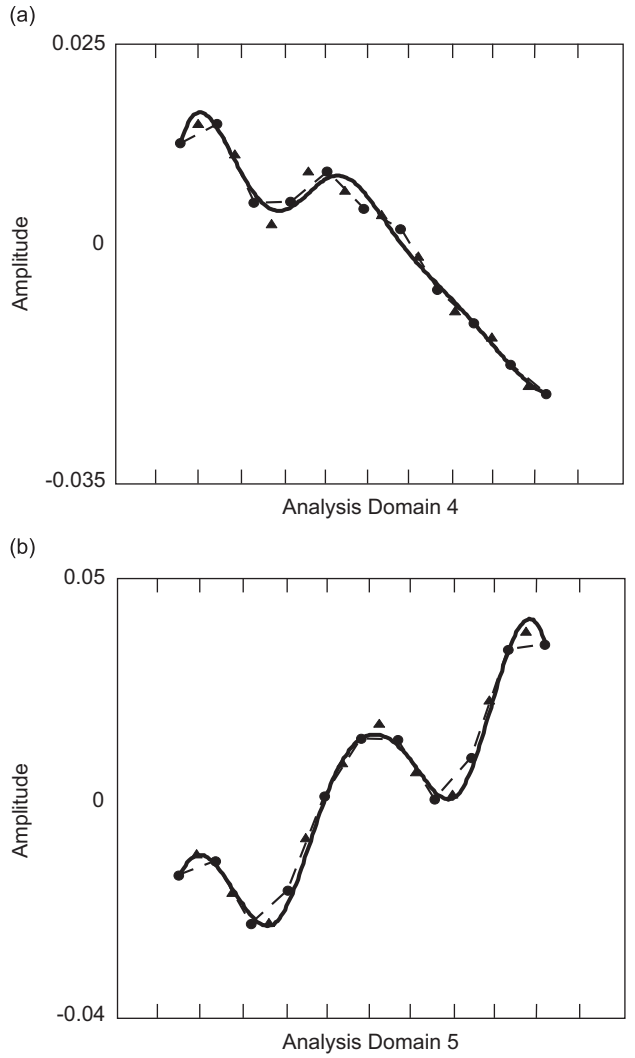

Fig. 6. Chosen predictors (amplitude in volts): (a) data and fifth-order predictor for domain 4, (b) data and fourth-order predictor for domain 5. ▲, Even data $\mathbf{X}_e$; – • –, odd data $\mathbf{X}_o$; ——, predictor.

vibration signal, $\bar{d}$ is the mean of the difference signal, and N the total number of data points in the time signal. From Eq. (8), it can be seen that FM4 is the normalized kurtosis of d. It is non-dimensional and designed to have a nominal value of 3 when d is purely Gaussian. For comparison, a metric using the CAL prediction error vector must be formed. Recall that the CAL prediction error vector for an individual tooth is denoted as φ. Thus, for a gear g with N_g teeth, let the prediction error vector φ for tooth P_n, $n = 1, \ldots, N_g$ be given as φ_n. The prediction error vector for the entire gear is then the concatenation of the individual φ_n, and is denoted $\mathbf{\Phi}$. The metric CAL4 can be formed by taking the normalized kurtosis of $\mathbf{\Phi}$. CAL4 is given as

$$\mathrm{CAL4} = \frac{N\sum_{i=1}^{N}(\mathbf{\Phi}_i - \bar{\mathbf{\Phi}})^4}{[\sum_{i=1}^{N}(\mathbf{\Phi}_i - \bar{\mathbf{\Phi}})^2]^2}, \tag{9}$$

where $\bar{\mathbf{\Phi}}$ is the mean of $\mathbf{\Phi}$ and N is the total number of data points in $\mathbf{\Phi}$. As with FM4, CAL4 is non-dimensional.

It is important to understand the underlying physical motivation for the formation of the CAL4 diagnostic metric. First consider the difference signal, d, used in FM4. The signal d is formed by subtracting an ideal

version of a transmission vibration signal based on a simple model of the transmission from the actual experimentally obtained signal. More specifically, d is a bandstop filtered signal, in which the stopbands are chosen based on the physical properties of the transmission under consideration. Thus, d contains frequencies that are considered to be physically meaningful only in the presence of damage. Otherwise, d is expected to contain only noise. Now, recall that in lifting, the prediction error preserves the higher order polynomial structure while the low-order structure is suppressed, which is equivalent to preserving the high-frequency signal characteristics. In CAL, the frequencies that are preserved in the prediction error vector are time varying, specifically, they vary from domain to domain. In addition, the frequencies which are preserved in $\mathbf{\Phi}$ are chosen based on the characteristics of the signal associated with the operation of the transmission, specifically, the conjugate action of the gear teeth. The set of bases model the vibration signal associated with healthy conjugate action, and thus, for a healthy transmission, the CAL prediction error is expected to contain only noise.

Thus, similar to d, $\mathbf{\Phi}$ can be considered to be a signal where frequencies that are physically meaningful only in the presence of damage are preserved while the frequencies associated with a healthy transmission are suppressed. The difference is in the technique used to form the model of a healthy transmission vibration signal. In $\mathbf{\Phi}$, a model based on an empirical signal is formed using CAL, while in d, a simple model of transmission vibrations is used. In addition, $\mathbf{\Phi}$ is based on individual tooth mesh waveforms errors while d is computed globally.

6. Experimental results

The vibration data used for this work was collected from the UMTTR shown in Fig. 7. The gearbox used in the UMTTR is an Emerson Power Transmission PlanetPower® single stage planetary reduction gearbox with a reduction ratio of 3.84:1, shown in Fig. 8. The ring gear has 71 teeth, the sun gear has 25 teeth, and each planet gear has 22 teeth. Vibrations are measured using PCB accelerometers mounted around the outside of the ring gear. They are then processed using the planetary gear vibration separation algorithm initially developed by McFadden and Howard [12,29,30]. The selection of the appropriate window for use with the vibration separation algorithm has been discussed extensively in the literature [3,9,31,32]. For this research, the window selected for use with the algorithm is a Tukey Window with a taper ratio of 4/5. This window has

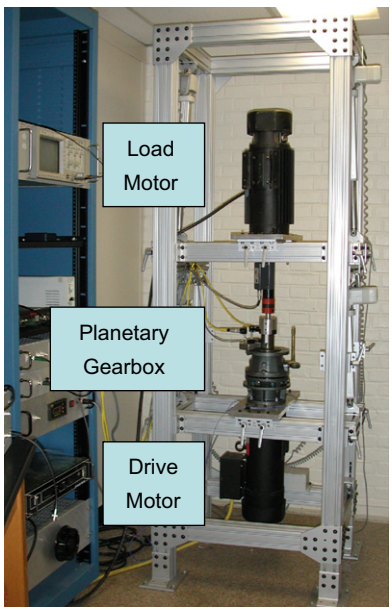

Fig. 7. University of Maryland transmission test rig.

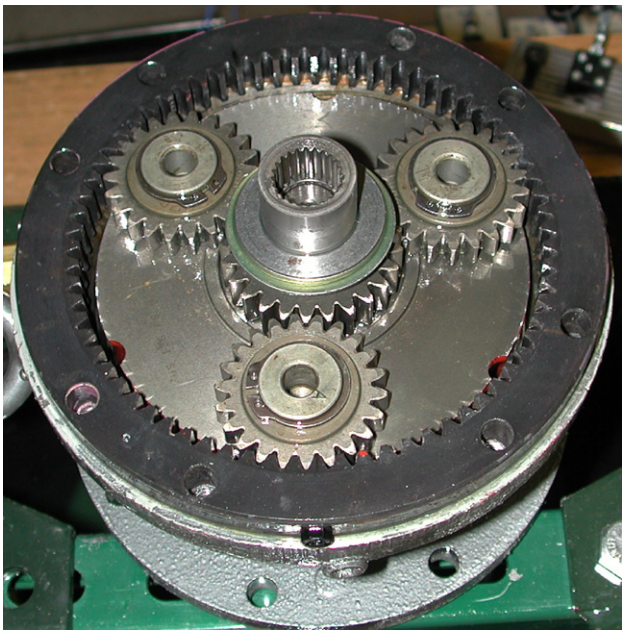

Fig. 8. Inside the PlanetPower® planetary reduction gearbox.

been shown to introduce minimal distortions in the tooth mesh waveform while effectively attenuating the discontinuities due to window assembly [9]. CAL was then applied to one set of healthy-state vibration signals under the low load condition and a predictor was found for each planet. Healthy-state vibration signals from the low, medium and high load conditions as well as the damaged-state vibration signals were then analyzed using CAL in conjunction with the previously chosen predictor. Finally, both FM4 and CAL4 are used to process the data and the results are compared.

6.1. Torque load variation

The effect of load variations on the output of the CAL diagnostic algorithm is of particular interest for helicopter transmission health monitoring due to large torque load fluctuations be seen by the main transmission caused by the varying flight conditions.

Currently, the UMTTR is limited in its ability to load the gearbox used for this investigation. The maximum rated output torque of the gearbox is 349.1 N m at 1750 rev/min. All experiments in this study are run at 1200 rev/min, and at this speed, the UMTTR can only drive the gearbox with an output torque ranging from 11.3 to 17.0 N m, nominally 3–5% of maximum. Consequently, all the loads in the torque load sensitivity study are in the low torque operating range of the gearbox. Thus, the load sensitivity study is not comprehensive, instead it only provides a general idea of the effect of varying load on the CAL prediction error.

Vibration data is collected from the gearbox operating under healthy-state conditions for nominal output torques of 11.3, 14.1, and 17.0 N m, referred to as low, medium and high loads, respectively. One set of low-load data is used to generate the CAL model, then separate sets of low-, medium-, and high-load data are processed using the model. The prediction error vectors are then compared.

Figs. 9–11 show the vibration signal, CAL prediction error and the FM4 and CAL4 values for each torque load. First, notice that the vibration signals for each of the planets exhibit different patterns. It is possible that the differences in the patterns are due to the low torque load. Next, consider the CAL prediction error. Note that a small coupling can be observed between load level and prediction error amplitude that manifests itself as an increase in the amplitude of the CAL prediction error with increasing torque.

Given that this coupling appears to be small, it is expected that it would not have a significant effect on the detection of the damage cases considered in this paper. However, since the range of load cases investigated

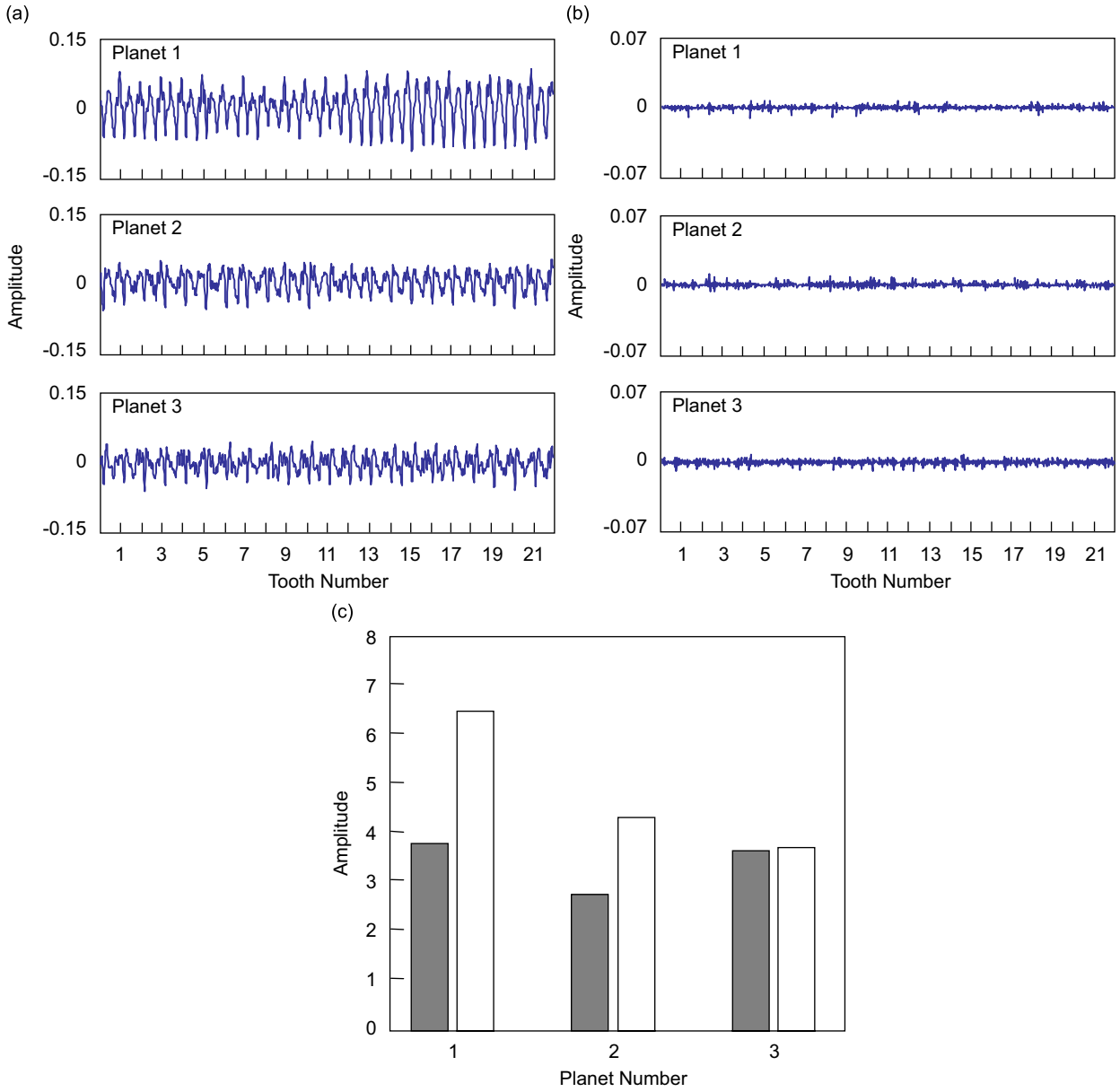

Fig. 9. Healthy state, low load: (a) separated vibration signals (V), (b) constrained adaptive lifting prediction error (V), and (c) FM4 versus CAL4. ■, FM4; □, CAL4.

is small, it cannot be determined from this study whether the coupling would become significant at higher loads.

To further investigate the effect of load, the CAL4 diagnostic metric is compared to the FM4 diagnostic metric. The results of this comparison are given in Figs. 9c, 10c, and 11c. Notice that FM4 appears to be relatively independent of load level, remaining relatively constant in a range from approximately 3 to 4. Recall that for Gaussian noise, FM4 should have a value of 3. However, in practice, the noise is never truly Gaussian. Thus for damage detection, an appropriate threshold must be set such that if the metric exceeds the threshold, then potential damage is indicated. In most cases, CAL4 also appears to be independent of torque load. The one exception is planet 1. For planet 1, CAL4 appears to increase consistently with increasing load. This possible coupling requires further investigation using a test rig that can load the gearbox to, or beyond,

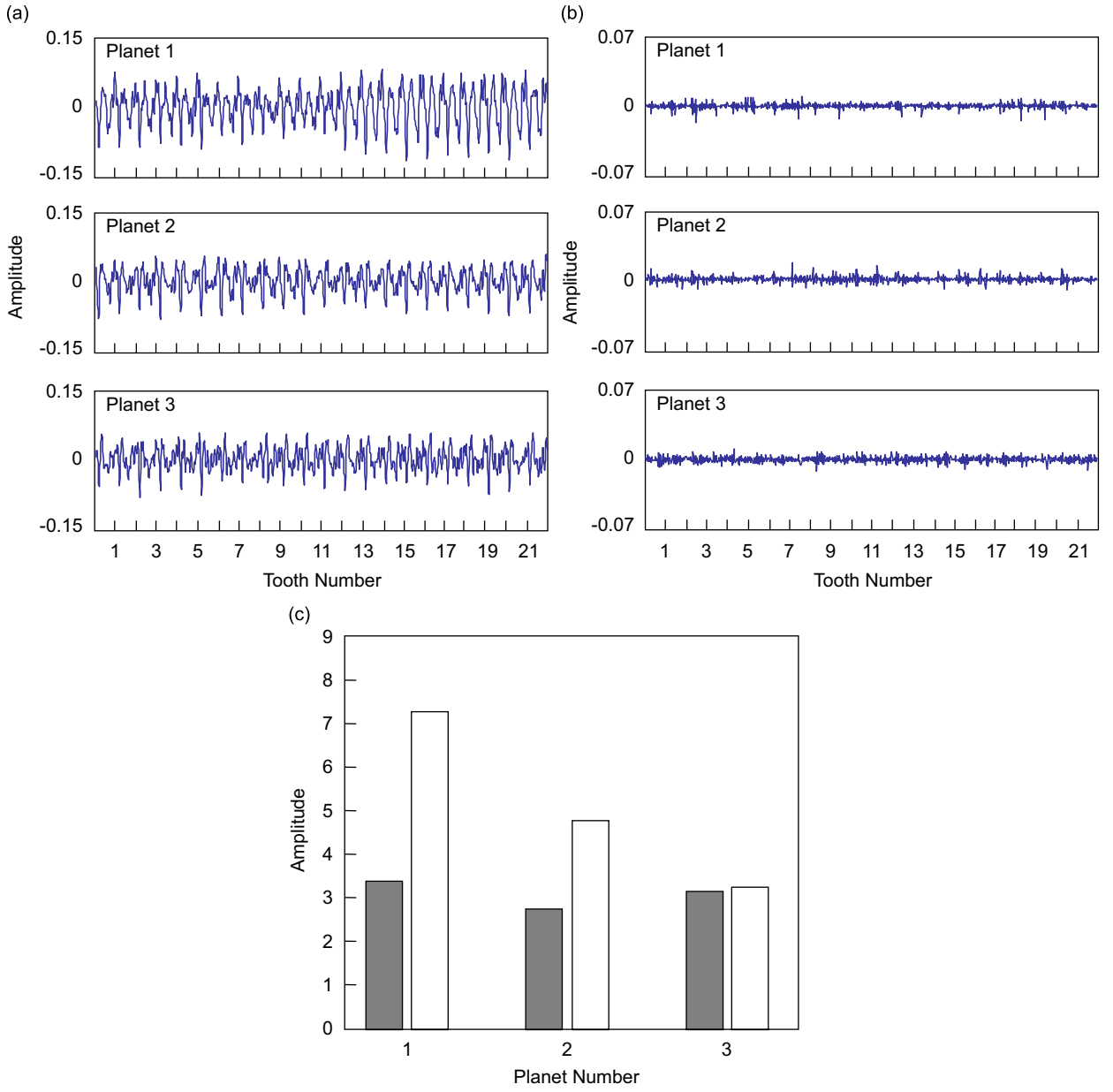

Fig. 10. Healthy state, medium load: (a) separated vibration signals (V), (b) constrained adaptive lifting prediction error (V), and (c) FM4 versus CAL4. ■, FM4; □, CAL4.

the maximum rated output torque. In addition, it should be noted that the CAL4 values for planet 1 are significantly higher that for planets 2 and 3. To understand this result, recall that the kurtosis is a measure of the peakedness of the distribution about the mean of the data under consideration. A closer inspection of the CAL prediction error vector reveals that for planet 1, a few spikes or outliers are present, while for planets 2 and 3, the distribution is more Gaussian. Thus, even though the amplitude of the prediction error vector is relatively small and consistent between planets, CAL4 is different. This may indicate that taking the kurtosis of the CAL error vector may not be the best method to quantify the result. Otherwise, separate thresholds may have to be set for each individual planets. Setting thresholds appropriately is an ongoing topic of research [33].

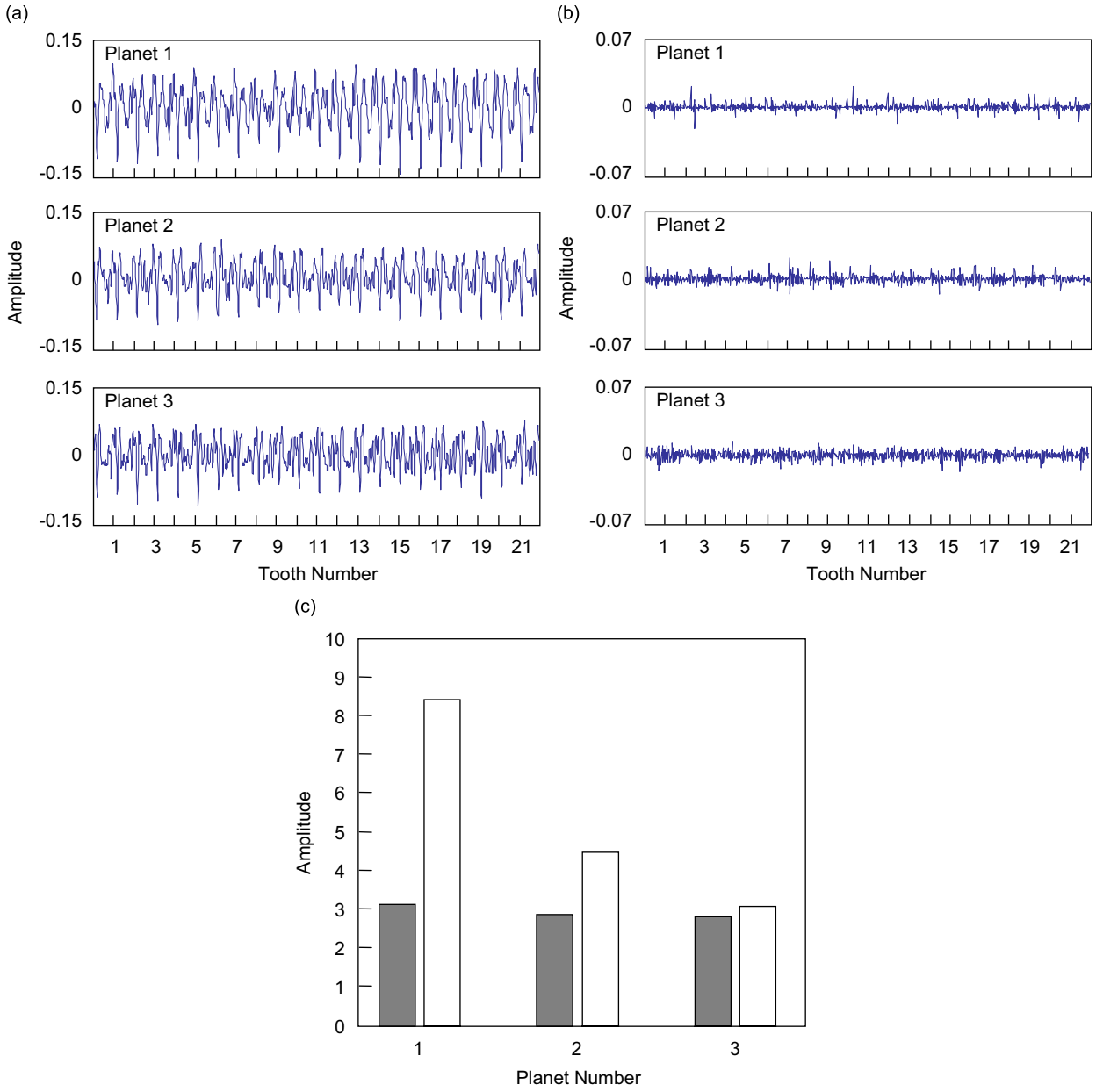

Fig. 11. Healthy state, high load: (a) separated vibration signals (V), (b) constrained adaptive lifting prediction error (V), and (c) FM4 versus CAL4. ■, FM4; □, CAL4.

6.2. Damage detection

For the damage detection investigation, vibration data is collected from the gearbox for both healthy and damaged states. A study presented by Wang and Wong [34] demonstrated that damage detection tends to be more difficult in the low torque range. Thus, the lowest output torque setting, 11.3 N m nominal, is used for the damage detection investigation. A subset of the healthy-state data is used to generate the CAL model. Data is collected from three damaged states: planet 2 with one tooth spalled, planet 2 with 5 consecutive teeth spalled, and planet 2 with all teeth spalled. Given that the UMTTR is incapable of loading the gearbox to failure, spalling is simulated by the removal of a small amount of material from a tooth face that meshes with

the ring gear. A healthy and damaged planet gear are shown in Fig. 12. In each case, planet 2 is placed in the gearbox and the position and rotation index are monitored in order to keep track of the location of the damaged teeth. In the first case, the damaged tooth is positioned such that the damage is expected to appear on tooth 18. In the second case, the damage is expected to appear on teeth 16–20.

Figs. 9 and 13–15 show the vibration signal, CAL prediction error and the FM4 and CAL4 values for each damage case in addition to the low-load healthy case. It should be noted that the gearbox exhibits some characteristics that complicate damage detection. In particular, the damage on planet 2 tends to slightly corrupt the planet 3 vibration signal and could lead to a false positive indication for planet 3. For example, the small spike observed on tooth 5 of planet 3 in Fig. 13 is a caused by the damage on planet 2. This phenomenon has been independently observed and may be a result of the low torque load used for this set of experiments. Further investigation into the cause of this coupling is required.

First consider the single tooth spalling case. The tooth spall on planet 2, tooth 18 is evident in the CAL prediction error vector as seen in Fig. 13b. This damage is noticeable even by direct inspection of the separated vibration signal, seen in Fig. 13a. In addition, an inspection of planets 1 and 3 reveals that separation was successful and that no damage is indicated on either planet 1 or 3. The damage is only evident on planet 2.

Next, consider the five-teeth spalled case. Once again, an inspection of the CAL prediction error clearly shows that the damage is located on teeth 16–20 of planet 2 as shown in Fig. 14b. In addition, it can be seen that planet 1 is clearly undamaged. Planet 3, on the other hand, is not as clear. An inspection of the planet 3 CAL prediction error vector shows evidence of corruption from the damage on planet 2. However, the short duration increases in the amplitude of the CAL output are small compared to those in planet 2. In addition they are wider, i.e. of longer duration, and thus are of a different nature than the damage. However, it is possible that these anomalies could lead to false positive detections.

Finally consider the all teeth spalled case. An inspection of the CAL prediction error vector shows that the damage is very evident on nearly every tooth of planet 2 as seen in Fig. 15b, whereas planet 1 shows no

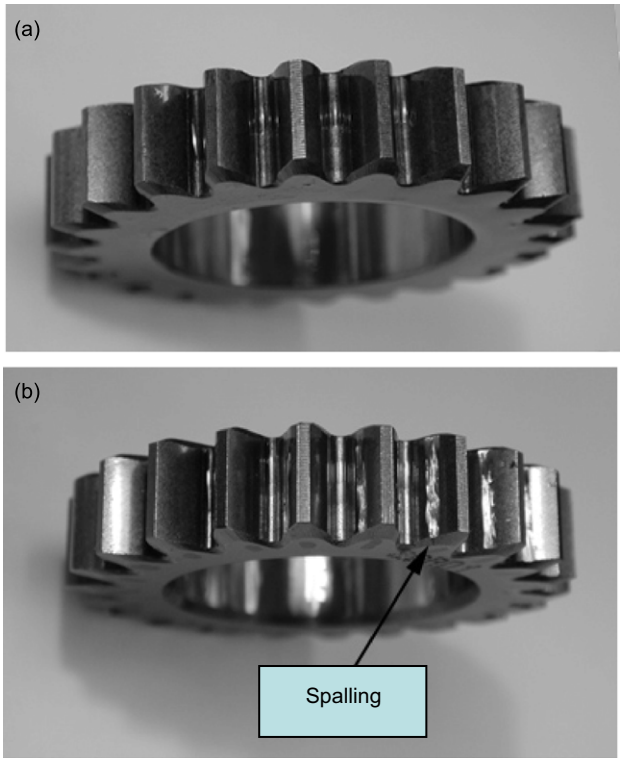

Fig. 12. Healthy- and damage-state planet gears: (a) healthy planet gear and (b) planet gear with all teeth spalled.

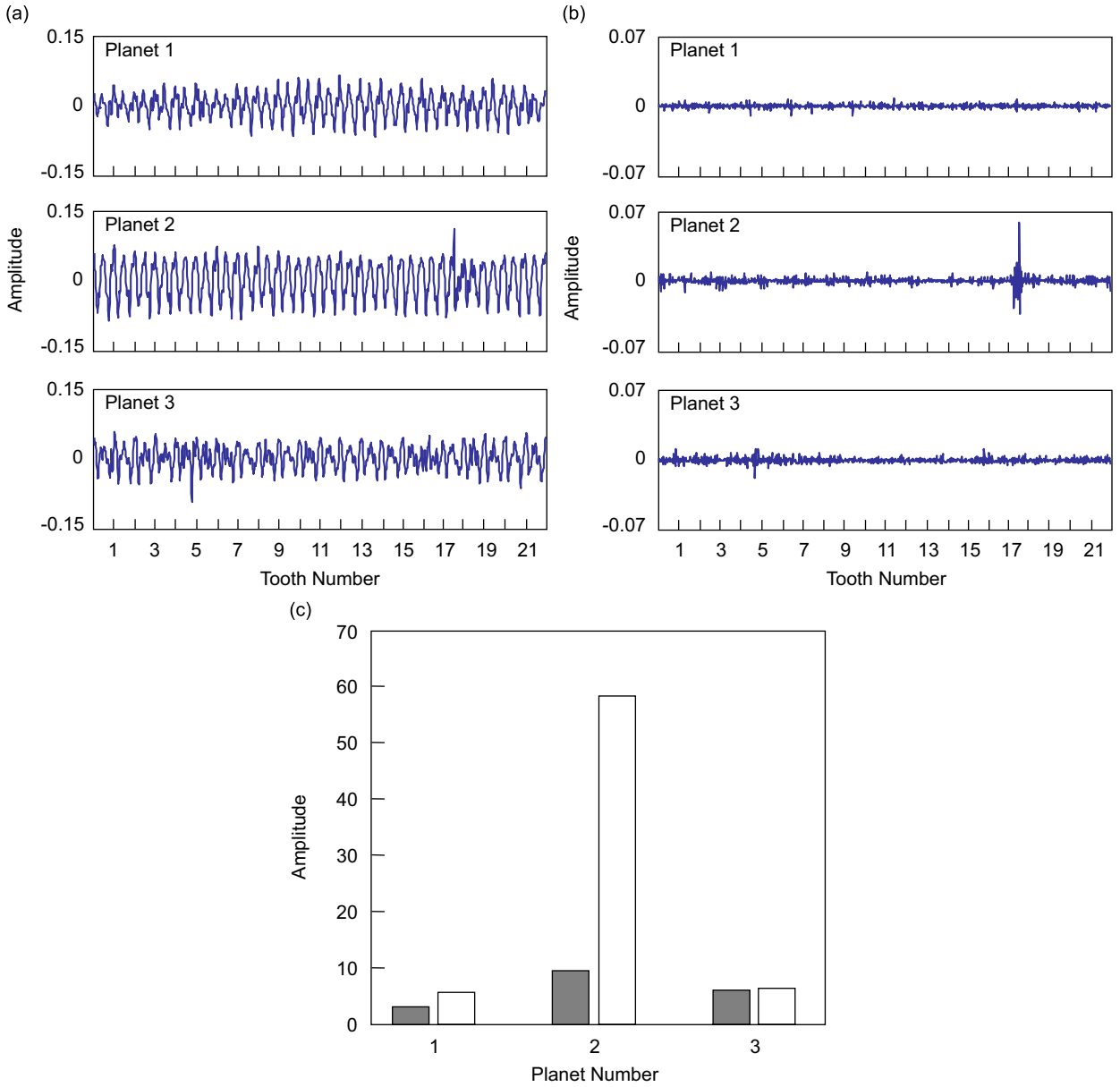

Fig. 13. One tooth spalled on planet 2: (a) separated vibration signals (V), (b) constrained adaptive lifting prediction error (V), and (c) FM4 versus CAL4. ■, FM4; □, CAL4.

increase in amplitude, and planet 3 shows only a small increase. Thus, distributed damage is clearly indicated in the CAL prediction error vector.

Next a comparison of the damage detection capabilities of CAL is compared with FM4. FM4, and CAL4 are calculated for each damage case, and the results are presented in Figs. 13c, 14c, and 15c. Notice that CAL4 always indicates damage on planet 2, although it is more sensitive to damage on a few teeth rather than all the teeth due to the distribution of the all teeth damaged case being more Gaussian than the one-tooth and five-teeth damaged cases, each of which only have a small number of large amplitude spikes in the data resulting in a more peaked distribution. FM4 also indicates damage on planet 2 in the one tooth spalled case and in the five-teeth spalled case. However, CAL4 is significantly more sensitive to the damage, particularly in the

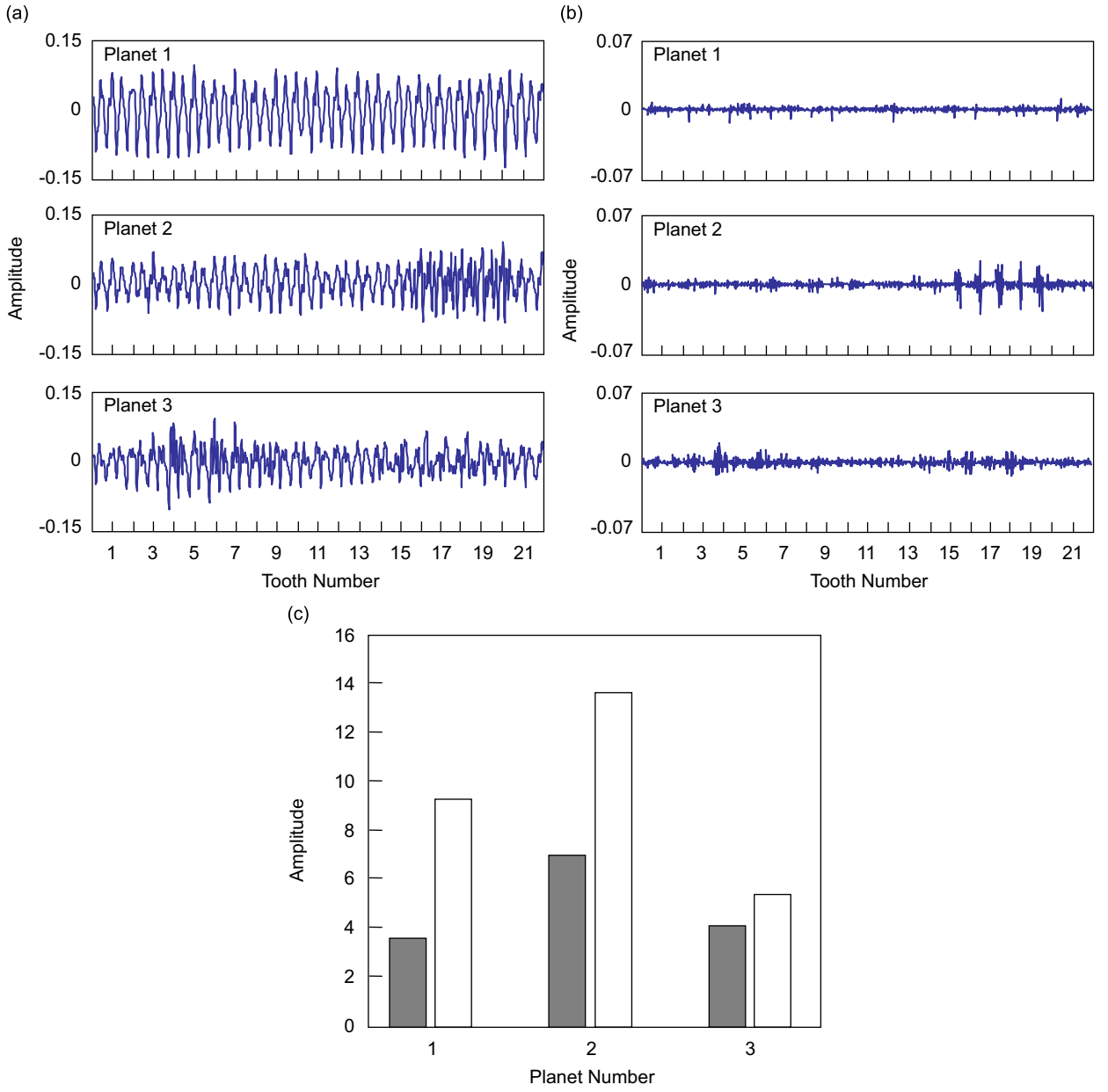

Fig. 14. Five teeth spalled on planet 2: (a) separated vibration signals (V), (b) constrained adaptive lifting prediction error (V), and (c) FM4 versus CAL4. ■, FM4; □, CAL4.

one-tooth spalled case. In the all teeth spalled case the damage on planet 2 is not sufficiently evident in the FM4 result. Thus, it can be seen that CAL4 outperforms FM4 in these cases.

These results show that CAL is potentially beneficial for transmission diagnostics. However, further investigation is required to better validate the performance of the algorithm.

7. Conclusion

In summary, this paper presents a new diagnostic approach, the time domain analysis of the individual tooth mesh waveforms using a signal adaptive time domain realization of the wavelet transform. First, the

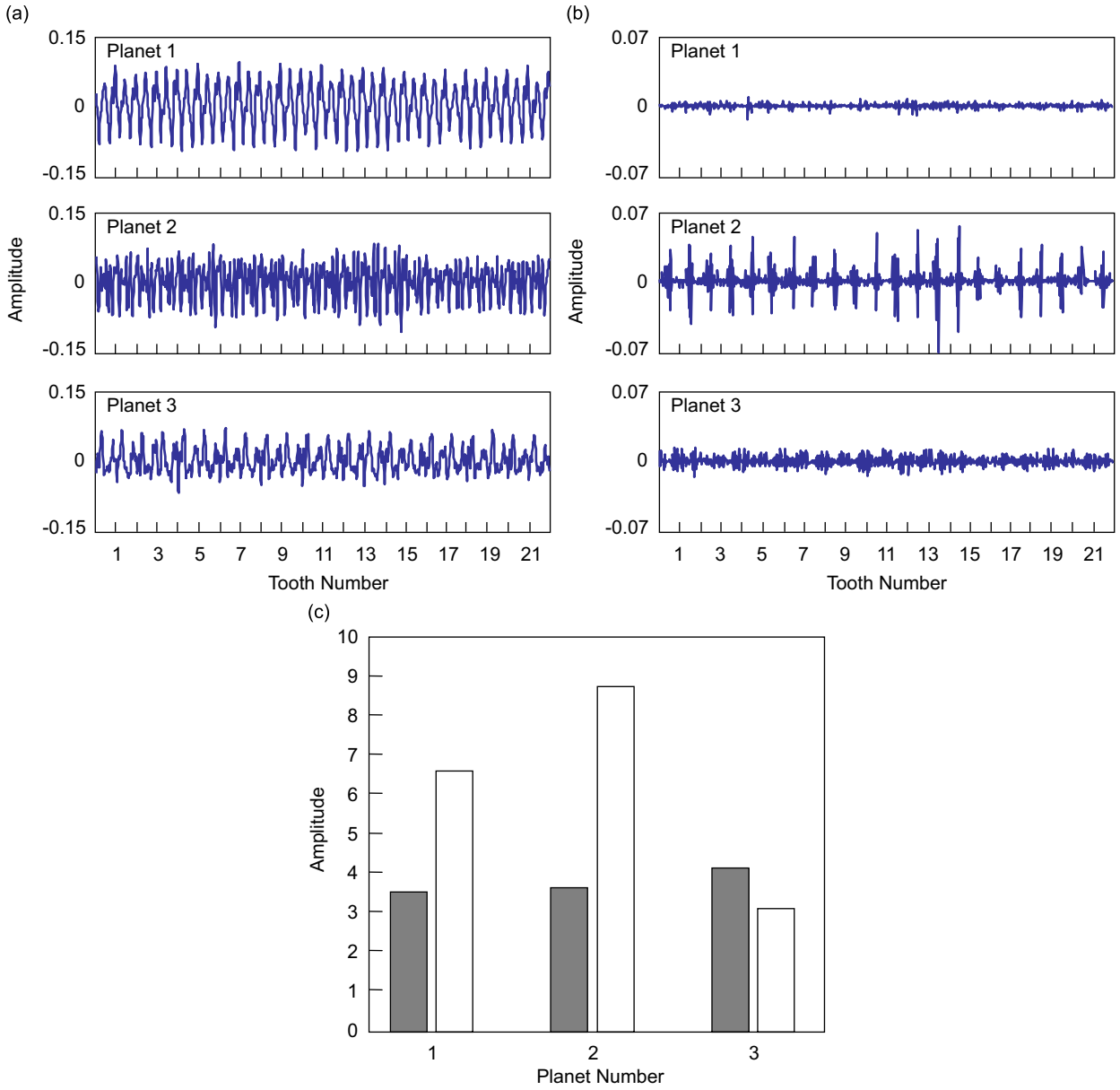

Fig. 15. All teeth spalled on planet 2: (a) separated vibration signals (V), (b) constrained adaptive lifting prediction error (V), and (c) FM4 versus CAL4. ■, FM4; □, CAL4.

analysis of the individual tooth mesh waveforms is discussed. The lifting scheme, a time domain prediction-error realization of the wavelet transform is summarized and the addition of adaptivity to lifting is presented. A modification of adaptive lifting, referred to as CAL, is developed to enhance observed changes in the vibration signal associated with the onset of individual tooth damage. Using the CAL prediction error vector, a damage detection metric CAL4 is developed based on the normalized kurtosis.

Next, an initial validation study of the CAL diagnostic algorithm focused on assessing the effect of load variations on the output and the damage detection capabilities of the technique is presented. CAL4 is then computed using each prediction error vector and the result is compared to the metric FM4. These results show that the CAL diagnostic algorithm is a promising new tool for planetary transmission diagnostics. However, further investigation is required to better validate the performance of the algorithm and determine the

potential for false positive indications or missed detections. Specifically, a more extensive validation study must be performed using a transmission test rig system that can load the gearbox under consideration to, or beyond, the maximum rated output torque. Subsequently, the performance of the algorithm should be validated using a transmission test rig that is more representative of a real helicopter transmission, such as the OH-58 transmission test rig located at the NASA Glenn Research Center [35].

Acknowledgments

This work is supported by the NASA Glenn Research Center, Contract no. NAG32223, with Dr. David G. Lewicki serving as contract monitor.

References

[1] P.D. Samuel, D.J. Pines, A review of vibration-based techniques for helicopter transmission diagnostics, *Journal of Sound and Vibration* 282 (1–2) (2005) 475–508.
[2] B. Liu, S. Ling, On the selection of informative wavelets for machinery diagnosis, *Mechanical Systems and Signal Processing* 13 (1) (1999) 145–162.
[3] P.D. Samuel, D.J. Pines, Planetary gear box diagnostics using adaptive vibration signal representations: a proposed methodology, *Proceedings of the American Helicopter Society 57th Annual Forum*, Washington, DC, 2001.
[4] P.D. Samuel, D.J. Pines, A planetary gearbox diagnostic technique using constrained adaptive lifting, *Proceedings of the DSTO Third International Conference on Health and Usage Monitoring—HUMS2003*, Melbourne, Australia, 2003, Paper no. 5.9, Included on CD-ROM.
[5] P.D. Samuel, D.J. Pines, Helicopter transmission diagnostics using constrained adaptive lifting, *Proceedings of the American Helicopter Society 59th Annual Forum*, Phoenix, AZ, 2003, pp. 351–361.
[6] W. Sweldens, The lifting scheme: a new philosophy in biorthogonal wavelet constructions, *Wavelet Applications in Signal and Image Processing III*, Proceedings of SPIE Vol. 2569, San Diego, CA, 1995, pp. 68–79.
[7] W. Trappe, K.J.R. Liu, Adaptivity in the lifting scheme, *Proceedings of the Conference on Information Sciences and Systems*, Baltimore, MD, 1999, pp. 950–955.
[8] R.L. Claypoole, R.G. Baraniuk, R.D. Nowak, Adaptive wavelet transforms via lifting, *Proceedings of the IEEE Conference on Acoustics, Speech, and Signal Processing*, Seattle, WA, 1998, pp. 1513–1516.
[9] P.D. Samuel, Helicopter Transmission Diagnostics Using Constrained Adaptive Lifting, PhD Thesis, University of Maryland, College Park, MD, USA, August 2003.
[10] L. Liu, Design Rules to Enhance Hums Sensitivity to Spur Gear Gaults, PhD Thesis, University of Maryland, College Park, MD, USA. February 2003.
[11] L. Liu, D.J. Pines, Sensitivity of vibration-based fault metrics to spur gear crack damage and diametral pitch, *Journal of the American Helicopter Society* 49 (3) (2004) 288–299.
[12] P.D. McFadden, A technique for calculating the time domain averages of the vibration of the individual planet gears and sun gear in an epicyclic gearbox, *Journal of Sound and Vibration* 144 (1) (1991) 163–172.
[13] W. Sweldens, P. Schröder, Building your own wavelets at home, in: *Wavelets in Computer Graphics*, *ACM SIGGRAPH Course Notes*, 1996, pp. 15–87.
[14] W. Sweldens, The lifting scheme: a custom-design construction of biorthogonal wavelets, *Applied Computational Harmonic Analysis* 3 (2) (1996) 186–200.
[15] C. Herley, M. Vetterli, Wavelets and recursive filterbanks, *IEEE Transactions on Signal Processing* 41 (8) (1993) 2536–2556.
[16] I. Daubechies, W. Sweldens, Factoring wavelet transforms into lifting steps, *Journal of Fourier Analysis and Applications* 4 (3) (1998) 245–276.
[17] A. Cohen, I. Daubechies, J. Feauveau, Bi-orthogonal bases of compactly supported wavelets, *Communications on Pure and Applied Mathematics* 45 (1992) 485–560.
[18] I. Daubechies, Time frequency localization operators: a geometric phase space approach, *IEEE Transactions on Information Theory* 34 (1988) 605–612.
[19] R.R. Coifman, M.V. Wickerhauser, Entropy-based algorithms for best-basis selection, *IEEE Transactions on Information Theory* 38 (1992) 713–718.
[20] S. Mallat, Z. Zhang, Matching pursuit with time–frequency dictionaries, *IEEE Transactions on Signal Processing* 41 (12) (1993) 3397–3415.
[21] S.S. Chen, D.L. Donoho, M.A. Saunders, Atomic decomposition by basis pursuit, *SIAM Journal on Scientific Computing* 20 (1) (1998) 33–61.
[22] R.L. Claypoole, G. Davis, W. Sweldens, R.G. Baraniuk, Nonlinear wavelet transforms for image coding, *Proceedings of the 31st Asilomar Conference on Signals, Systems, and Computers*, Vol. 1, Pacific Grove, CA, 1997, pp. 662–667.
[23] E. Jones, P. Runkle, N. Dasgupta, L. Carin, Signal adaptive wavelet design using genetic algorithms, *Wavelet Applications VII, Proceedings of SPIE*, Vol. 4056, Orlando, FL, 2000, pp. 362–371.

[24] P.D. Samuel, D.J. Pines, Adaptive signal representations for helicopter transmission diagnostics, *Proceedings of the Third International Workshop on Structural Health Monitoring*, Stanford, CA, 2001, pp. 221–230.
[25] C.H. Reinsch, Smoothing by spline functions, *Numerische Mathematik* 10 (1967) 177–183.
[26] C. de Boor, *A Practical Guide to Splines*, Springer, New York, NY, 2001.
[27] S.G. Mallat, *A Wavelet Tour of Signal Processing*, second ed., Academic Press, New York, NY, 1999.
[28] R.M. Stewart, Some useful analysis techniques for gearbox diagnostics, *Technical Report MHM/R/10/77*, Machine Health Monitoring Group, Institute of Sound and Vibration Research, University of Southampton, July 1977.
[29] P.D. McFadden, I.M. Howard, The detection of seeded faults in an epicyclic gearbox by signal averaging of the vibration, *Technical Report ARL-PROP-R-183*, Aeronautical Research Laboratory, Australian Department of Defence, October 1990.
[30] I.M. Howard, An investigation of vibration signal averaging of individual components in an epicyclic gearbox, *Technical Report ARL-PROP-R-185*, Aeronautical Research Laboratory, Australian Department of Defence, March 1991.
[31] P.D. McFadden, Window functions for the calculation of the time domain averages of the vibration of the individual planet gears and sun gear in an epicyclic gearbox, *Journal of Vibration and Acoustics* 116 (1994) 179–187.
[32] D. Forrester, A method for the separation of epicyclic planet gear vibration signatures, *Proceedings of Acoustical and Vibratory Surveillance Methods and Diagnostic Techniques*, Senlis, France, 1998, pp. 539–548.
[33] P.J. Dempsey, M. Mosher, E.M. Huff, Threshold assessment of gear diagnostic tools on flight and test rig data, *Proceedings of the American Helicopter Society 59th Annual Forum*, Phoenix, AZ, 2003, pp. 1244–1262.
[34] W. Wang, A.K. Wong, A model-based gear diagnostic technique, *Technical Report DSTO-TR-1079*, Defence Science and Technology Organisation, Australian Department of Defence, December 2000.
[35] D.G. Lewicki, H.J. Decker, J.T. Shimski, Development of a full-scale transmission testing procedure to evaluate advanced lubricants, *Technical Report NASA TP-3265, AVSCOM TR-91-C-026*, NASA and the US Army Aviation Systems Command, August 1992.